Contents lists available at ScienceDirect

Food and Bioproducts Processing

journal homepage: www.elsevier.com/locate/fbp

Effect of particle size on *in vitro* intestinal digestion of emulsion-filled gels: Mathematical analysis based on the Gallagher–Corrigan model

Claudia González[a], *Ricardo Simpson*[a,c], *Oscar Vega*[e,f], *Valeria del Campo*[b], *Marlene Pinto*[a], *Lida Fuentes*[c], *Helena Nuñez*[a], *Ashley K. Young*[d], *Cristian Ramírez*[a,c,*]

[a] *Departamento de Ingeniería Química y Ambiental, Universidad Técnica Federico Santa María, P.O. Box 110-V, Valparaíso, Chile*
[b] *Departamento de Física, Universidad Técnica Federico Santa María, P.O. Box 110-V, Valparaíso, Chile*
[c] *Centro Regional de Estudios en Alimentos Saludables (CREAS), CONICYT-Regional GORE Valparaíso Proyecto R17A10001, Avenida Universidad 330, Placilla, Curauma, Valparaíso, Chile*
[d] *Department of Food, Bioprocessing, and Nutrition Sciences, North Carolina State University, Raleigh, NC, United States*
[e] *BIOALI Research Group, Department of Food, Faculty of Pharmaceutical Sciences and Food, Universidad de Antioquia, Medellín, Colombia*
[f] *Corporación Universitaria Americana, Medellín, Colombia*

ARTICLE INFO

Article history:
Received 17 June 2019
Received in revised form 16 December 2019
Accepted 17 December 2019
Available online 26 December 2019

Keywords:
Oil/water emulsion
In vitro digestion
pH-stat method
Particle size distribution
Gallagher-Corrigan model
Lipid digestion

ABSTRACT

Free fatty acid (FFA) release from the *in vitro* digestion of an emulsion-filled gel using three different particle size distributions and its modeling using the Weibull function and Gallagher–Corrigan model were investigated. To produce the emulsion-filled gel, an oil/water mix was prepared and blended with sodium alginate to finally produce small calcium alginate gel cubes. Three different particle size area distributions were generated by comminuting the cubes applying 5, 10, and 15 cycles of compression/shearing. The particles were intestinally *in vitro* digested, and the fraction of FFA released was calculated and analyzed using the Weibull function and Gallagher–Corrigan model. The FFA release showed a sigmoidal behavior for the three particle distributions; the Weibull function did not show a good fit. The Gallagher–Corrigan model presented a good fit to the FFA data, reinforced with a random error distribution. The model parameters were able to explain the kinetic processes related to both surface emulsion release and emulsion release by matrix dissolution. In addition, some parameters were linearly correlated ($R^2 > 0.99$) with particle size, which established a relationship between particle size and the kinetics of release attained during the first stage of the digestion curve.

1. Introduction

Polysaccharide gelation has been extensively studied, as it contributes to the structural and textural properties of a wide range of food products. Using polysaccharides to manipulate food structure can enable food nutrient protection and lipid digestion control (Li et al., 2011; Parada and Aguilera, 2011; Mishra and Monro, 2012; Ramírez et al., 2015; Guo et al., 2017; Corstens et al., 2017; Chen et al., 2018).

* Corresponding author at: Departamento de Ingeniería Química y Ambiental, Universidad Técnica Federico Santa María, P.O. Box 110-V, Valparaíso, Chile.
E-mail address: cristian.ramirez@usm.cl (C. Ramírez).
https://doi.org/10.1016/j.fbp.2019.12.009
0960-3085/

Lipid digestion in oil/water emulsions (O/W) is an interfacial process involving pancreatic lipase and colipase adsorption on the surface of emulsified oil droplets (Wooster et al., 2014; Corstens et al., 2017). For conventional O/W emulsions, lipid digestion is dependent on factors such as interfacial properties, oil phase surface area, oil accessibility, and the ratio of the oil to the lipase/bile salts (Guo et al., 2017). Therefore, one approach for delaying lipolysis is to limit lipase access to the oil droplet by building a biopolymer-based network around the oil droplets, *i.e.*, structuring an emulsion-filled gel. Wooster et al. (2014) studied the effect of food structure on lipid digestion using different biopolymer networks during emulsion structuring. A simple biopolymer network was found to have a considerable effect on structure formation and food emulsion digestion. Guo et al. (2017) suggested that the emulsion-filled gel structure delays enzyme and salt diffusion, as they must pass through the continuous phase to access the droplet surface. In addition, the gel structure plays an important role in determining both gel texture and/or viscosity. Corstens et al. (2017) suggested that a nondigestible gel matrix is preferable for achieving greater control over lipase diffusion; possible candidates include dietary fibers such as chitosan and alginate (Rodríguez and Albertengo, 2005; Corstens et al., 2018). However, a gel matrix not only influences lipid digestion by delaying lipase diffusion to the oil droplets, but it is also likely to require chewing to prepare it for swallowing. Therefore, the particle size distribution generated during oral processing may play an important role in determining lipid digestion rate and extent (Bourne, 2004; Miquel-Kergoat et al., 2015; Cassady et al., 2009).

When an emulsion is part of a polymeric matrix, the oil droplets can be released from the matrix and digested in the medium because of a diffusion process. Then, the oil droplet diffuses to the medium because of a degradation process of the matrix, which has been reported in studies performed in biomedical research of drug release (Gallagher and Corrigan, 2000; Mucha et al., 2014). In this sense, the use of an empirical model that describes the release or digestive process can be quite helpful for developing foods with customized behavior. For example, Guo et al. (2017) applied the Weibull function to describe a typical emulsion digestion process. The time exponent of the Weibull model was useful to describe the process. The model states that obtaining a value of $\beta > 1$ suggests that lipid digestion occurs in three phases: 1) early slow digestion, because of the effect of the food matrix; 2) rapid digestion during the intermediate stage, because of the breakdown of the matrix; and 3) gradual digestion during the final stage, as most of the oil has already been hydrolyzed. Conversely, $\beta < 1$ shows that lipid digestion occurs in two phases: 1) initial rapid digestion, because of the structure surrounding the oil droplet breaking down, and 2) subsequent gradual digestion.

Another empirical approach is the Gallagher–Corrigan model (Gallagher and Corrigan, 2000), which has been used to describe the sigmodal release process that occurs during *in vitro* digestion of a microencapsulated drug in polymeric matrices. The model has the advantage that it simultaneously includes two process that typically occur during *in vitro* digestion of an encapsulated drug and that it can be applied to lipid digestion. The first part is related to oil droplet oil digestion that is near the surface of the matrix, and the second part is related to lipid digestion of oil droplets released from the gel because of a matrix degradation (Balcerzak and Mucha, 2010). This model has typically been used during the drug release process, but not in lipid digestion incorporated into a biopolymeric matrix (Gorrasi et al., 2017).

Thus, the aim of this study was to evaluate the effect of particle size distribution on intestinal *in vitro* digestion of an emulsion-filled gel using the Weibull function and Gallagher–Corrigan model to establish the relationship between the particle size and model parameters.

2. Materials and methods

2.1. Materials

Edible vegetable oil (99% soybean oil, 1% palm oil; Chef, Chile), Tween 80 (Chemix, Greece), sodium alginate (Loba Chemie, Chile), calcium chloride dihydrate (Merck, Germany), porcine pancreatic lipase Type II L3126 (Sigma Aldrich, Germany), porcine bile extract B8631 (Sigma Aldrich, Germany), sodium chloride, sodium hydroxide, sodium phosphate monobasic, and sodium phosphate dibasic were provided by GA Ventas, Chile.

2.2. Methods

2.2.1. Oil/water (O/W) emulsion preparation

The emulsion was prepared with 36 g soy oil with 4 g of Tween 80 and 60 g of distilled water which were homogenized at 20,000 rpm for 10 min using an Ika T25 basic homogenizer equipped with a S25N-25F dispersion tool (Ika, Staufen, Germany) (Muhamad et al., 2016; Perrechil and Cunha, 2010). To complete the emulsion process, the solution was sonicated at 350 W for 60 s (Qsonica Q700, Qsonica Sonicators, USA) (Silva et al., 2013). The emulsion was cooled at 4 °C and adjusted to pH 7 using NaOH 0.15 M.

2.2.2. Emulsion-filled alginate gel cubes (model food)

The model food was developed following the work of Ramírez et al. (2019) with some modifications. 136 g oil/water emulsion was mixed with 1500 mL 2 wt.% sodium alginate solution at 20 °C. The mixture was then spread carefully over a plastic mould (330 × 220 × 35 mm deep) on top of 1500 mL 2.0 M CaCl2. This stratified arrangement was kept at 20 °C for 48 h, to allow ion exchange to form the calcium alginate gel. The emulsion-filled calcium alginate gel was then removed and placed on a tray beneath a cutting system which cut out, simultaneously, 100 cuboids with cross-section 12.5 × 12.5 mm^2. The height of individual gel cubes was trimmed to 12.5 mm by manual cutting with a scalpel.

2.2.3. Determination of particle size and zeta potential of the oil/water emulsions

The oil droplet size distribution and the emulsion zeta potential were determined using a dynamic light scattering system (Nanosizer ZS90, Malvern Instruments, UK). Samples were prepared by diluting 0.1 mL of emulsion with 9.9 mL distilled water and the required amount charged to a cuvette. Measurements were made at 25 °C. Droplet size distribution and z-potential were calculated using the Zetasizer V7.11 software (Malvern Instruments, UK). The refractive index was set at 1.460 and the dispersant (water) at 1.333 (Corstens et al., 2017; Liu et al., 2006). Both characterizations were performed in triplicate.

2.2.4. Uniaxial compression test of the model food

Uniaxial compression tests were performed to determine the hardness of the emulsion-filled alginate gel cubes using a CTS Texture Analyzer (Brookfield, Toronto, Canada) running the TexturePro CT V1.2 software. The test was based on the method proposed by Muñoz et al. (1986). An individual gel cube (12.5 × 12.5 × 12.5 mm) was placed face down on a plate and compressed at 0.3 mm s^{-1} with a cylindrical probe of acrylic (50 mm diameter) until the gel broke. The hardness was expressed in N and was obtained from the force-displacement curve. Testing was performed in triplicate.

2.2.5. Mechanical reduction of the emulsion-filled alginate gel cube size

Mechanical compression coupled with a shear system was designed to reduce the particle size of the emulsion-filled alginate gel cubes and produce a particle size distribution similar to that produced during oral processing (Ramírez et al., 2019). A single emulsion-filled alginate gel cube (12.5 × 12.5 × 12.5 mm) was placed between two plates (diameter = 20 mm) and was subjected to 5, 10, or 15 cycles of compression (force = 30 N) and a 5° shear angle during each compression. A 30-N compression force was selected based on Mioche and Peyron (1994). This analysis was conducted in triplicate.

2.2.6. Determination of the particle size distribution of compressed emulsion-filled alginate gel samples

The particle size distribution of the compressed emulsion-filled alginate gel samples was determined using a flatbed scanner (600-dpi resolution, CanonScan LiDE110; Canon Inc, Vietnam). Images were saved in a **.tiff form, and particle processing and quantification were performed using the Image-Pro-Plus software (Media Cybernetics, Rockville, USA) (Ramírez and Aguilera, 2011). The image processing consisted of converting the image from 24 to 8 bits (grayscale) and then segmenting the image based on histogram segmentation. The resulting binary image was used to quantify the particle area (mm^2) of the gel samples after 5, 10, or 15 compressions.

Particle area data were used to obtain a cumulative area fraction curve based on the number of particles. A particle size analysis was performed using the Rosin–Rammler model (Eq. (1)) to describe the cumulative size distribution of particles obtained after compression (Olthoff et al., 1984; Van der Bilt et al., 1993) as follows:

$$Q = 1 - \exp\left[-\left(\frac{x}{x_{50}}\right)^{2} \cdot \ln 2\right] \quad (1)$$

where x is the sieve class (mm^2), x_{50} is the theoretical sieve size (mm^2) through which 50% of the particles pass, b is the parameter indicating the broadness of the distribution (corresponding to the slope of the cumulative curve; increases in this value indicate a narrower particle size distribution), and Q is the fraction of the number of particles with a diameter less than x (Hutching et al., 2011).

The parameters x_{50} and b were obtained by nonlinear fitting of the real cumulative particle size distribution to the Rosin–Rammler model using the Solver Tool (Excel, Microsoft, USA).

2.2.7. In vitro intestinal digestion using pH-stat

In vitro intestinal digestion of the emulsion-filled alginate gel was performed using a pH-stat titrator (Mettler Toledo G20s, Greifensee, Switzerland) following the method proposed by Li and McClements (2010) with some modifications. Fifty emulsion-filled gel cubes (equivalent to 70 mL of emulsion-alginate solution or 1.89 g of soybean oil) were added to a flask containing 52.5 mL of bile extract solution (2625 mg of bile salt dispersed in a pH 7 phosphate buffer), 3.5 mL of $CaCl_2$ solution (575 mM in distilled water) and 3.5 mL of NaCl solution (5625 mM in distilled water). The final solution was adjusted to pH 7 using 0.15 M NaOH and heated to 37 °C using a thermoregulated bath. To start digestion, 5.25 mL of fresh lipase (315 mg of lipase in 5.25 mL of pH 7 phosphate buffer) was added. The titration was conducted using 0.15 M NaOH with pH 7 as the end point.

To quantify lipolysis, the free fatty acid release fraction (FFA) over time (2 h) was determined using Eq. (2) (Li and McClements, 2010) as follows:

$$FFA = \frac{V_{NaOH} * C_{NaOH} * MW_{oil}}{weight_{oil} * N} \quad (2)$$

where V is the volume (L) of the titrant used, C is the titrant concentration (NaOH, 0.15 mol/L), MW_{oil} is the molecular weight of the soybean oil (920 g/mol), $weight_{oil}$ is the mass of the soybean oil (1.90 ± 0.10 g) present in the emulsion, and N is the number of FFAs (N = 2) released from each triacylglycerol molecule.

2.2.8. Mathematical analysis of FFA release profiles: Weibull function and Gallagher–Corrigan model

The Weibull distribution function, commonly used to describe drug release profiles during *in vitro* analysis (Papadopoulou et al., 2006), was used to model the FFA release as follows:

$$F(t) = F_{max}\left(1 - e^{-kt^{\beta}}\right) \quad (3)$$

where F(t) is the FFA released during digestion at time t, F_{max} is the maximum fraction of FFA released during 120 min, k is the time scale of the process (h^{-1}) associated with the rate of FFA release, and β is a shape parameter that characterizes the shape of the release curves (Guo et al., 2017).

The Gallagher–Corrigan model (Gallagher and Corrigan, 2000) describes the levamisole (antihelminthic drug) release from a biodegradable biopolymer, which occurs during a biphasic process, with an initial fast release phase followed by a slower polymer degradation controlled release phase. The model presents the combination of two consecutive first-order kinetic mechanisms (the dual-mode diffusion model) with some modification introduced as follows (Balcerzak and Mucha, 2010; Gorrasi et al., 2017):

$$F(t) = b + Y_1\left(1 - e^{-k_1 t}\right) + Y_2\left(\frac{e^{k_2(t - kt_{max})}}{1 + e^{k_2(t - t_{max})}}\right) \quad (4)$$

where F(t) is the fraction of FFA released during digestion time t, Y_1 is the fraction of FFA released during the first stage, Y_2 is the fraction of FFA released during the second stage, k_1 is the first-order kinetic constant (h^{-1}) (first stage of release), k_2 is the kinetic constant for the second stage of the release process-matrix degradation and t_{max} is the time of the maximum fraction of the FFA release rate (h) (Balcerzak and Mucha, 2010).

The FFA release profiles in this study were modeled using Weibull functions and the Gallagher–Corrigan model. The Weibull and Gallagher–Corrigan model parameters were calculated for the emulsion and the emulsion-filled alginate gel

cubes after 5, 10, and 15 compression cycles, respectively. All the parameters were obtained by nonlinear regression of the data by minimizing the sum of squares error (SSE) using the Solver Tool (Excel, Microsoft) (Ramírez et al., 2019).

3. Results and discussion

3.1. *Characterization of the emulsions and emulsion-filled alginate gels*

The soybean oil O/W emulsion had a mean droplet size of 108 ± 5 nm. Silva et al. (2013) reported similar results (80–120 nm) for corn oil in water and olive oil in water emulsions prepared under similar conditions. The zeta potential values for the emulsion (−21.0 ± 2.0 mV) indicate a stable emulsion.

The emulsion-filled alginate gel hardness was found to be 16.26 ± 1.58 N. This value is within the range reported by Roopa and Bhattacharya (2008) for a calcium alginate gel system – the hardness of gels in that study ranged between 14 and 200 N depending on the $CaCl_2$ concentration, pH, and temperature. In terms of commercial products, the emulsion-filled gels are comparable to gummy bear hardness values reported in the literature (15.7 and 20.5 N (Shimadzu, 2012)).

3.2. *Particle size distribution of the compressed emulsion-filled alginate gels*

Fig. 1A shows the particle size distribution of the emulsion-filled gel after 5, 10, and 15 compression cycles. Increasing the number of compression cycles from 5 to 15 shifted the peak of the particle size distribution towards smaller particle sizes. However, 10 compression cycles produced a distribution with two maximum peaks at approximately 100 and 200 mm^2. In addition, the 5 and 10 compression cycles had similar particle size distribution ranges with values between 14.6 to 394 mm^2. Conversely, the range for 15 cycles was lower, with values between 10.5 to 292.3 mm^2.

Fig. 1B shows the Rosin–Rammler model-characterized cumulative particle size distribution curves for the emulsion-filled alginate gel after 5, 10, and 15 compression cycles. The particle size results are summarized in Table 1. When 50 gel cubes were individually comminuted using 5 cycles, the number of particles increased to 61. After a total of 15 cycles, it had increased further to 191 particles. Uncompressed samples had a particle area of 156.25 mm^2. The particle area range was similar for the 5 and 10 compression cycles (14.6–394.7 mm^2). However, increasing to 15 cycles lowered the particle area range to values between 10.5 and 292.3 mm^2. The Rosin–Rammler parameters show that increasing the number of compression cycles decreased the x_{50} values, as expected. This reduction was significant ($p < 0.05$), with values of 216.16, 152.36, and 88.83 mm^2 for 5, 10, and 15 cycles, respectively. The nonparametric statistical analysis of the particle size distribution data, based on a Kolmogorov-Smirnov test, showed significant differences between the three cumulative curves ($p < 0.05$).

3.3. *Analysis of FFA release during in vitro digestion of emulsion-filled gels*

Figs. 2 and 3 show the FFA release profiles for the O/W emulsion and emulsion-filled alginate gel compressed 5, 10 and 15 times fitted with the Weibull and Gallagher–Corrigan models, respectively. The highest triglyceride hydrolysis was observed

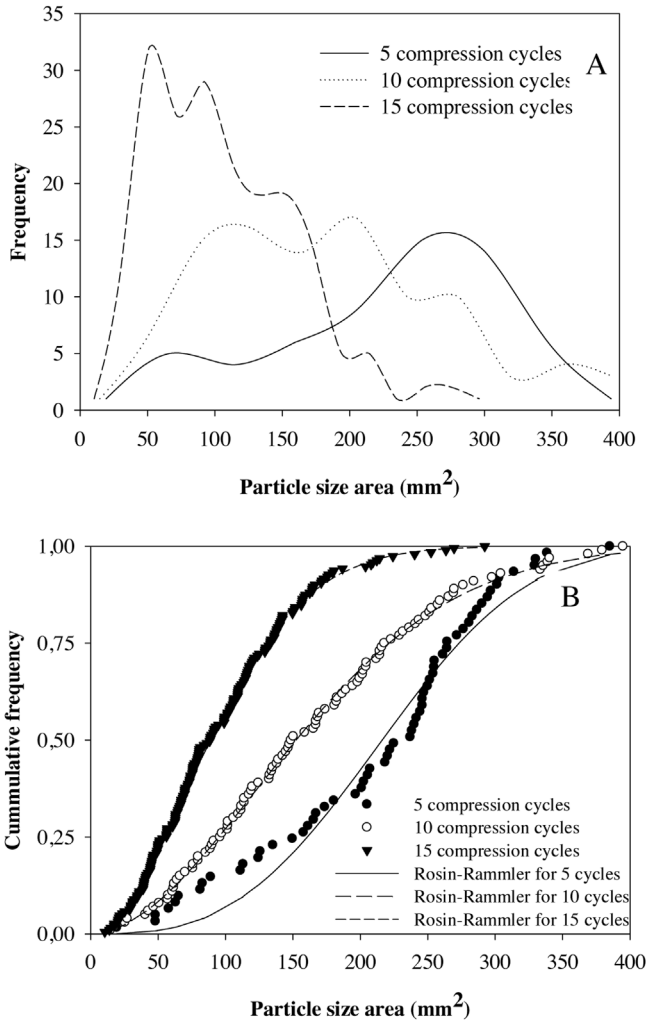

Fig. 1 – Particle size area distribution (mm^2) obtained for 50 emulsion-filled alginate gel cubes (12.5 × 12.5 × 12.5 mm) individually comminuted using 5, 10, or 15 compression cycles and then pooled for analysis (the analysis was performed in triplicates) A) Particle size area distribution (mm^2); B) cumulative particle size area distribution (mm^2) fitted using a Rosin–Rammler model.

for the O/W emulsion with 74% of FFA released. Similar results have been reported in the literature for intestinal *in vitro* digestion studies using O/W emulsions stabilized by whey protein isolates. Corstens et al. (2017) reported near 80% FFA release for a sunflower oil O/W emulsion and Guo et al. (2017) reported 90% FFA release for a canola oil O/W emulsion.

In general, this *in vitro* intestinal digestion study indicates that structuring a gel around emulsion droplets results in delayed FFA release. For all the emulsion-filled alginate gels, the FFA release (the gradient of the FFA release curves) during the first 30 min of the *in vitro* digestion process was slower than O/W emulsions. This slow release may be associated with the calcium alginate gel structure around the oil droplet but also with the dissolution of the alginate gel at pH 7, promoting the release of calcium ions and alginate into the medium. Li et al. (2011) reported a sigmoidal-shaped FFA release curve for emulsions with high calcium levels (20 mM). The authors attributed the suppression of FFA release to calcium promoting oil droplet the flocculation, thus inhibiting lipase access to the oil droplet surface. Interestingly, Li et al. (2011) showed the change in the slope of the digestion curve was at approximately 30 min following a similar trend to that observed in

Table 1 – Particle size analysis performed using the Rosin–Rammler model nonparametric statistics.

Emulsion-filled alginate compressed cubes	Number of particles**	Range of areas*	Rosin–Rammler parameters			
			X_{50} (mm^2)	b	SSE	R^2
Emulsion-filled alginate gel compressed 5 cycles	61	19.3–384.9	216.16[a]	2.96	0.161	0.9865
Emulsion-filled alginate gel compressed 10 cycles	100	14.6–394.7	152.36[b]	1.86	0.013	0.9993
Emulsion-filled alginate gel compressed 15 cycles	191	10.5–292.3	88.83[c]	1.83	0.006	0.9990

* Different letters indicate significant differences using a Kolmogorov–Smirnov non-parametric test ($p < 0.05$) between size distribution curves.
** Number of particles correspond to the total of particles obtained after mechanical compression.

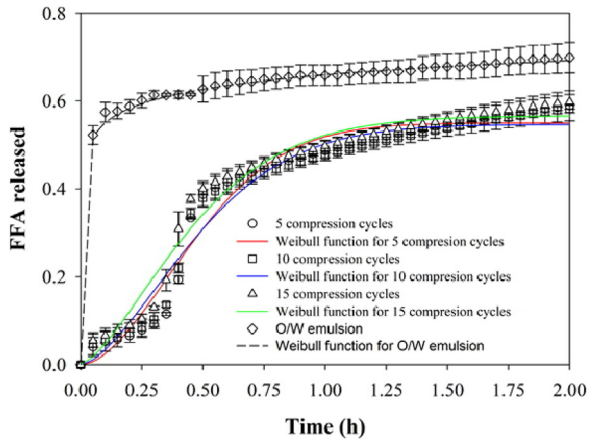

Fig. 2 – Fraction of free fatty acid release from the O/W emulsion and particles of emulsion-filled alginate gel fitted using the Weibull function.

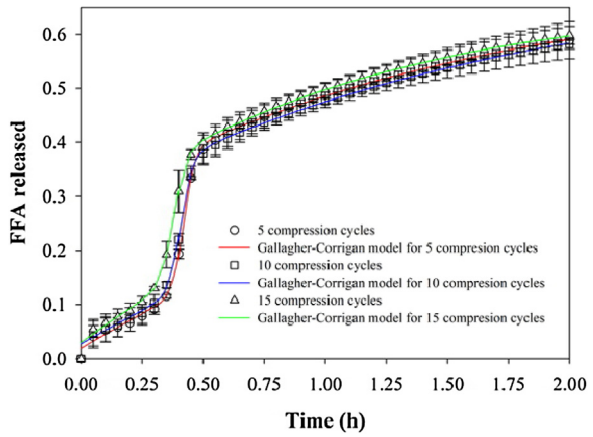

Fig. 3 – Fraction of free fatty acid release from the O/W emulsion and particles of emulsion-filled alginate gel fitted using the Gallagher–Corrigan model.

our study. Similar results have been reported for other non-digestible hydrocolloids, such as guar gum; the addition of 4 %w/w guar gum to a canola oil/water emulsion reduced lipid hydrolysis from 40 to 20% FFA release after 2 h of *in vitro* digestion. This was attributed to a viscosity effect; the formation of a viscous network decreases the molecular diffusion rates, resulting in delayed transport of the molecules to lipid particle interfaces (Amyoony et al., 2017). Another explanation for the differences in %FFA at 120 min between the emulsion with sodium alginate and the emulsion-filled alginate gel could be that the progressive dissolution of alginate gel particles into the medium allows for a slow increment in viscosity, which was not possible in the case of the emulsion with sodium alginate in which the viscosity remained the same during digestion.

3.4. *Mathematical analysis of FFA release profiles using the Weibull function and Gallagher–Corrigan model*

As can be observed in Table 2A, the modeling of FFA release through the Weibull function was adequate for the emulsion and with better adjustment (R^2) than that of the case of compressed emulsion-filled gels. For the emulsion, k and β showed values of 1.178 h^{-1} and 0.128, respectively (R^2 = 0.9939), with a sum of square error (SSE) of 0.0001. O/W emulsions presented $\beta < 1$ values, indicating that the digestion was initially rapid but leveled off at a lower FFA release rate (Guo et al., 2017).

For the three particle size distributions of emulsion-filled alginate gel cubes, the constants F_{max}, k and β were obtained. The values of F_{max} were near 1, without significant differences among the compression cycles applied. k values decreased from 2.694 to 2.418 h^{-1} as the number of compression cycles increased, but without significant differences. β values were greater than 1, varying from 1.851 for 5 compression cycles to 1.416 for 15 compression cycles. In general, when the model is empirical, it is difficult to establish some relationships or to explain constant behavior. However, the results show that as the particle size decreases, both k and β tend to be lower because the behavior tends to be more similar to that attained by O/W emulsion. Through a visual and statistical analysis of the goodness of fit of the release profile with the Weibull function, it is possible to conclude that the Weibull function is not adequate to model the sigmoidal behavior, mainly because it cannot explain the dissolution phenomena of an alginate gel during digestion.

In this sense, the model proposed by Gallagher–Corrigan through the combination of two phenomena, initial surface lipid hydrolysis followed by FFA release because of the polymer degradation mechanism, was more suitable to represent the hydrolysis behavior. Originally, the model proposed by Gallagher and Corrigan (2000) was developed to explain the mechanism involved in drug release from polymer matrices. However, in the case of an emulsion-filled alginate gel it was possible to observe the same mechanistic problem. The results obtained certainly confirm that initially there is a burst of the O/W emulsion to the medium because of the fracture process of the compression cycles that was quickly hydrolyzed. Then,

Table 2A – Weibull function parameters obtained during *in vitro* digestion for the O/W emulsion and emulsion-filled gel particles.

Compression cycles	Weibull function parameters				
	F_{max}	k	β	SSE	R^2
O/W	1.000 ± 0.000	1.178 ± 0.032	0.128 ± 0.010	0.0001	0.9939
5	0.557^a ± 0.025	2.694^a ± 0.317	1.851^a ± 0.110	0.0011	0.9841
10	0.550^a ± 0.008	2.454^a ± 0.137	1.572^b ± 0.090	0.0010	0.9830
15	0.565^a ± 0.012	2.418^a ± 0.261	1.416^b ± 0.088	0.0009	0.9853

*Different vowel letters indicate significantly differences $p < 0.05$.

Table 2B – Gallagher–Corrigan model parameters obtained during *in vitro* digestion for the O/W emulsion and emulsion-filled gel particles.

	Gallagher–Corrigan parameters							
Compression cycles	*b*	Y1	Y2	T_{max}	k_1	k_2	SSE	R^2
5	0.0259^a ± 0.0113	0.430^a ± 0.041	0.166^a ± 0.020	0.451^a ± 0.054	0.518^a ± 0.028	45.137^a ± 3.817	0.00001	0.9998
10	0.0417^a ± 0.0081	0.445^a ± 0.010	0.200^a ± 0.008	0.416^a ± 0.011	0.605^a ± 0.097	41.855^a ± 2.124	0.00002	0.9997
15	0.0410^a ± 0.0048	0.418^a ± 0.017	0.201^a ± 0.029	0.384^a ± 0.018	0.847^b ± 0.015	44.428^a ± 3.642	0.00001	0.9998

*Different vowel letters indicate significantly differences $p < 0.05$.

the hydrolysis continues with the emulsion released from the particle surface to the medium, which continues with the emulsion release because of biopolymer degradation Table 2B show the values obtained for the Gallagher–Corrigan-fitted parameters. The results show that the model was adequately fitted to the sigmodal release profile of the FFA, with values of SSE $<2 \times 10^{-5}$. Notably, this behavior (sigmoidal) has been widely reported in the *in vitro* drug release process incorporated in polymeric matrices (Gorrasi et al., 2017; Balcerzak and Mucha, 2010). The values of the burst constant (*b*-value), related to the emulsion that was not inside the particles and, therefore, available to be quickly converted to FFA, increased as the particle size decreases. For the *b*-value, the FFA fraction was 0.0259, 0.0417 and 0.0410 for 5, 10 and 15 compression cycles, respectively. Thus, as the compression cycles increase, the particle size decreases and therefore more emulsion was free in the medium, significantly increasing the value of the burst hydrolysis after 5 compression cycles.

The Y_1-value, related to the fraction of FFA released during the first stage of the FFA curve, remained from approximately 0.418 to 0.445, and non-significant differences were observed for the different compression cycles ($p > 0.05$). The Y_2-value related to the fraction of FFA released during the second stage of the FFA release curve showed that the value increased from 0.166 for 5 cycles to 0.201 when 15 compression cycles were applied ($p < 0.05$). Thus, as the particle size decreased the FFA fraction released was higher during the second stage. Regarding t_{max}, which is related to the time to the maximum FFA release rate (h), the results indicated that as the particle size decreases the t_{max} was lower, varying from 0.451 h for 5 cycles to 0.384 h for 15 cycles, which was because of the particle size reduction.

Analyzing the results obtained for k_1 it was possible to note that particle size has a significant effect on this constant. Thus, for 5 compression cycles, the k_1 was 0.518 h^{-1} and the value increased until 0.847 h^{-1} when 15 cycles were applied. Clearly, small particles favor the first-order kinetic behavior during the first stage, which is related to the emulsion release from the surface particle. The relationship between particle area and volume plays an important role in FFA release. Finally, the kinetic constant k_2, related to the second stage of the release process, specifically to the matrix degradation, the values remained from approximately 41.86–45.14 h^{-1}, without significant differences for 5, 10 and 15 compression cycles.

Certainly, particle size distribution attained after compressing 5, 10 or 15 times affected the behavior of the FFA release profile, which was adequately fitted (R^2) using the Gallagher–Corrigan model. An error analysis was completed to further confirm the suitability of the Gallagher–Corrigan model. In fact, the error distribution was much more randomly distributed and nearer zero for the Gallagher–Corrigan model than that for the Weibull function for the three particle size distributions (Fig. 4). Analyzing the parameters that were affected by particle size such as t_{max} and k_1, it was possible to find a linear relationship between these parameters and particle size (represented by x_{50}), with R^2 values of 0.9998 and 0.9635, respectively.

4. Conclusions

This study highlighted how the presence of a semisolid biopolymeric matrix, based on a nondigestible carbohydrate, could delay FFA release through sigmodal behavior and reduce the amount of FFA released from an emulsion-filled gel during *in vitro* digestion. The results obtained show that the continually digested emulsion attained values near 80% of the FFA, while the digestion of the emulsion-filled alginate gels yielded a sigmoidal-shaped FFA release profile with FFA values of approximately 60%. Two mechanisms were clearly defined, mechanisms I and II, in which mechanism I was clearly defined by the particle size distribution. Considering this FFA release behavior, the Weibull function was not a suitable model for the process. However, the Gallagher-Corrigan model presented a better goodness of fit and its suitability was reinforced with a random error distribution. The Gallagher–Corrigan model parameters were capable of describing both mechanisms involved in the *in vitro* intestinal digestion process. Linear relationships were found between

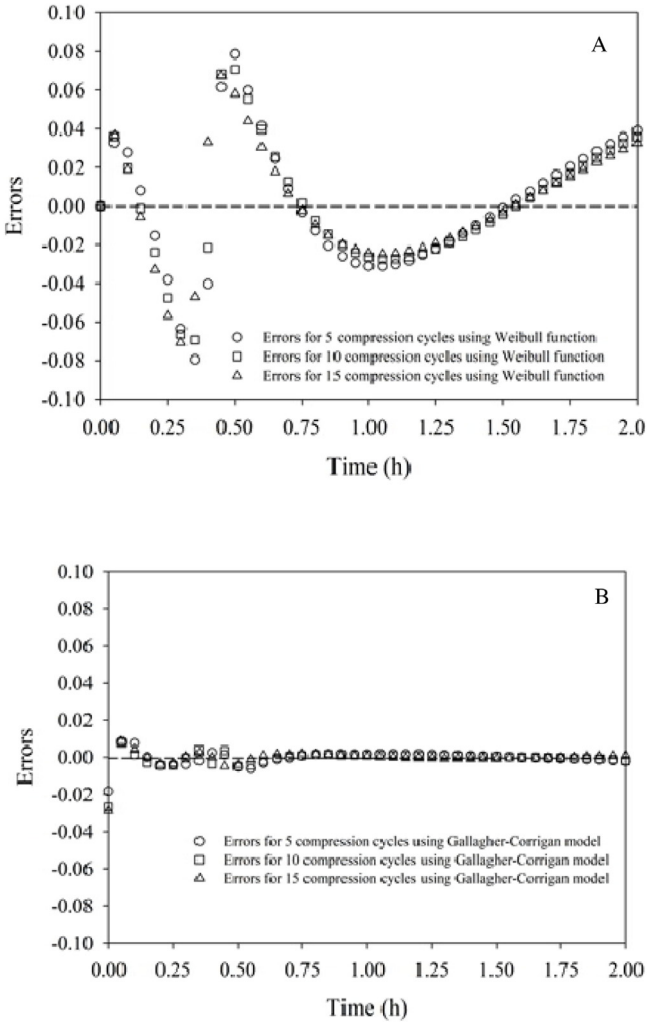

Fig. 4 – Error distribution for the FFA fraction obtained using particles with 5, 10 and 15 compression cycles fitted to the A) Weibull function and B) Gallagher–Corrigan model.

the particle size and some kinetic parameters, such as t_{max} and k_1. Finally, the number of compression cycles, which affected the particle size distribution as occurs during the chewing process, did not affect the fraction of FFA released; however, it did affect the kinetics involved during the process.

Declaration of interests

The authors declare that they have no known competing financial interests or personal relationships that could have appeared to influence the work reported in this paper.

Acknowledgements

The authors are grateful for the financial support provided by CONICYT through the FONDECYT project 1160811 and 1191280 (Cristian Ramírez) and FONDECYT project 1181270 (Ricardo Simpson).

Appendix A. Supplementary data

Supplementary material related to this article can be found, in the online version, at doi:https://doi.org/10.1016/j.fbp.2019.12.009.

References

Amyoony, J., Lin, X., Wright, A.J., 2017. GG decreases in vitro digestive lipolysis and carotenoid bioaccesibility from a pre-formed protein-stabilized emulsion. Bioact. Carbohydr. Diet. Fibre 9, 21–27.

Bourne, M., 2004. Relation between texture and mastication. J. Texture Stud. 35, 125–143.

Balcerzak, J., Mucha, M., 2010. Analysis of model drug reléase kinetics from complex matrices of polylactide-chitosan. Prog. Chem. Appl. Chitin Deriv. XV, 117–126.

Cassady, B.A., Hollis, J.H., Fulford, A.D., Considine, R.V., Matters, R.D., 2009. Mastication of almonds: effects of lipid bioaccesibility, appetite, and hormone response. Am. J. Clin. Nutr. 89, 794–800.

Chen, F., Deng, Z., Zhang, Z., Zhang, R., Xu, Q., Fan, G., Luo, T., McClements, D.J., 2018. Controlling lipid digestion profiles using mixtures of different types of microgel: alginate beads and carrageenan beads. J. Food Eng. 238, 156–163.

Corstens, M.N., Berton-Carabin, C.C., Elichiry-Ortiz, P.T., Hol, K., Troost, F.J., Masclee, A., Schroën, K., 2017. Emulsion-alginate beads designed to control in vitro intestinal lipolysis: towards appetite control. J. Funct. Foods 34, 319–328.

Corstens, M.N., Berton-Carabin, C.C., Schroën, K., Viau, M., Maynier, A., 2018. Emulsion encapsulation in calcium-alginate beads delays lipolysis during dynamic in vitro digestion. J. Funct. Foods 46, 394–402.

Gallagher, K.M., Corrigan, O.I., 2000. Mechanistic aspect of the release of levamisole hydrocholoride from biodegradable polymers. J. Control. Release 69, 261–272.

Gorrasi, G., Attanasio, G., Izzo, L., Sorrentino, A., 2017. Controlled release mechanisms of sodium benzoate from a biodegradable polymer and halloysite nanotube composite. Polym. Int. 66, 690–698.

Guo, Q., Bellissimo, N., Rousseau, D., 2017. Role of gel structure in controlling in vitro intestinal lipid digestion in whey protein emulsions gels. Food Hydrocoll. 69, 264–272.

Hutching, S., Foster, K.D., Bronlund, J., Letle, R., Jones, J.R., Morgenstern, M.P., 2011. Mastication of heterogeneous foods: peanuts inside two different food matrices. Food Qual. Prefer., 332–339.

Li, Y., McClements, D., 2010. New mathematical model for interpreting pH-stat digestion profiles: impact of lipid droplet characteristics on in vitro digestibility. J. Agric. Food Chem. 58, 8085–8092.

Li, Y., Hu, M., McClements, D.J., 2011. Factor affecting lipase digestibility of emulsified lipids using an in vitro digestion model: proposal for a standardized pH-stat method. Food Chem. 126, 498–505.

Liu, W., Sun, D., Li, C., Liu, Q., Xu, J., 2006. Formation and stability of paraffin oil-in-water nano-emulsions prepared by the emulsion inversion point method. J. Colloid Interface Sci., 557–563.

Mioche, L., Peyron, M.A., 1994. Bite force displayed during assessment of hardness in various texture contexts. Arch. Oral Biol. 40 (5), 415–423.

Miquel-Kergoat, S., Azais-Braesco, V., Burton-Freeman, B., Hetherington, M., 2015. Effects of chewing on appetite, food intake and gut hormones: A. Physiol. Behav. 151, 88–96.

Mishra, S., Monro, J., 2012. Wholeness and primary and secondary food structure effects on *in vitro* digestions patterns determine nutritionally distinct carbohydrate fractions in cereal foods. Food Chem. 135, 1968–1974.

Mucha, M., Socha-Michalak, I., Balcerzak, J., 2014. Biodegradable polymers as matrices for control drug reléase. Adv. Mater. Res. 911, 336–341.

Muhamad, I.I., Quin, C.H., Selvakumaran, S., 2016. Preparation and evaluation of water-in-soybean oil-in-water emulsions by repeated premix membrane emulsification method using cellulose acetate membrane. J. Food Sci. Technol. 53, 1845–1855.

Muñoz, A., Pagborn, R., Noble, A., 1986. Sensory and mechanical attributes of gel texture. II. Gelatin sodium alginate and kappa-carrageenan gels. J. Texture Stud. 1, 17–36.

Olthoff, L.W., van der Bilt, A., Bosman, F., Kleizen, H.H., 1984. Distribution of particle size in food comminuted by human mastication. Arch. Oral Biol. 29, 899–903.

Papadopoulou, V., Kosmidis, K., Vlachou, M., Macheras, P., 2006. On the use of the Weibull function for the discernment of drug release mechanisms. Int. J. Pharm. 309, 44–50.

Parada, J., Aguilera, J., 2011. Microstructure, mechanical properties, and starch digestibility of a cooked dough made with potato starch and wheat gluten. LWT-Food Sci. Technol. 44 (8), 1739–1744.

Perrechil, F.A., Cunha, R.L., 2010. Oil-in-water emulsions stabilized by sodium caseinate: influence of pH, high-pressure homogenization and locust bean gum addition. J. Food Eng. 97, 441–448.

Ramírez, C., Aguilera, J., 2011. Determination of a representative area element (RAE) based on nonparametric statistics in bread. J. Food Eng. 102, 197–201.

Ramírez, C., Millón, C., Nuñez, H., Pinto, M., Valencia, P., Acevedo, C., Simpson, R., 2015. Study of effect of sodium alginate on potato starch digestibility during *in vitro* digestion. Food Hydrocoll. 44, 328–332.

Ramírez, C., Millón, C., Nuñez, H., del Campo, V., Almonacid, S., Simpson, R., 2019. Effect of particle size distribution on the in vitro digestion of calcium alginate-starchy model foods. J. Food Process Eng., e13097.

Shimadzu, Retrieved from 2012. Chewing properties of gummy bears test. SHIMADZU EUROPA GmbH, Duisburg, Germany http://www.amse.it/wp-content/uploads/2016/09/LAAN_A_AG.pdf.

Roopa, B.S., Bhattacharya, S., 2008. Alginate gels: I. characterization of textural attributes. J. Food Eng. 85, 123–131.

Rodríguez, M.S., Albertengo, L.E., 2005. Interaction between chitosan and oil under stomach and duodenal digestive chemical conditions. Biosci. Biotechnol. Biochem. 69, 2057–2062.

Silva, A.E., Barratt, G., Chéron, M., Egito, E.S., 2013. Development of oil-in-water microemulsions for the oral delivery of amphotericin B. Int. J. Pharm. 454, 641–648.

Van der Bilt, A., van der Glas, H.W., Mowlana, F., Heath, M.R., 1993. A comparison between sieving and optical scanning for determination of particle size distribution obtained by mastication in man. Arch. Oral Biol. 38, 159–162.

Wooster, T.J., Day, L., Xu, M., Golding, M., Oiseth, S., Keogh, J., Clifton, P., 2014. Impact of different biopolymer networks on the digestion of gastric structured emulsion. Food Hydrocoll. 36, 102–114.